Final report
42691-PH-QC
Using electrons on a helium film as qubits

John Goodkind
Physics Department
UCSD

1 The system

1.1 General properties of electrons on helium,

Electrons, with energy less than 1 eV, when sprayed onto the surface of liquid helium become bound to the surface by the electrostatic image charge in the liquid. Their mobility along the surface is extremely high so that their motion in the plane is essentially unbound. This means that each electron is in a potential like that of a 1D hydrogen atom.

The Schrödinger equation for these states is

$$\frac{\partial^2\psi}{\partial z^2}+\frac{2m}{\hbar^2}\left(\frac{\Lambda e^2}{z}+E\right)\psi=0 \qquad (1)$$

Where $\Lambda=\frac{\kappa-1}{4(\kappa+1)}=6.95\times10^{-3}$ and $\kappa=1.05723$ is the dielectric constant of liquid helium. The normalized ground state wave function and energy for this Hamiltonian is

$$\psi_0=\frac{2}{a^{3/2}}zExp[-z/a] \qquad E_0=\frac{-\hbar^2}{2ma^2}=-\frac{e^2\Lambda}{2a}=-9.2\text{ K} \qquad (2)$$

Where $a=\frac{\hbar^2}{m\Lambda e^2}=7.64$ nm is the Bohr radius

The first excited state wave function and energy are

$$\psi_1=\frac{1}{\sqrt{2}}\frac{1}{a^{3/2}}\left(z-\frac{1}{2a}z^2\right)Exp[-\frac{z}{2a}] \qquad E_1 = E_0/4 \qquad (3)$$

The energy level difference between these states has been measured using microwave spectroscopy[1]. In addition the form of the potential was tested by measuring tunneling rates of the electrons when an external electric field was applied to pull the electrons from the surface[2]. The energy difference is $E_1 - E_0 = 120$ GHz. For qubit testing and operations an electrostatic field is applied so that $E_1 - E_0$ may be tuned in and out of resonance with microwaves at 140 GHz.

The system is physically very clean and simple so that, other than relaxation processes, numerical solutions of the Schrodinger equation for various operating conditions of the qubits accurately represent the expected operation. We simulated, numerically, one and two qubit gates to explore the limits of adiabatic change of state as the rate of change of DC and microwave fields was increased. The switch from adiabatic to rapid changes was shown to occur at rates much higher than can be achieved and much

Report Documentation Page

Form Approved
OMB No. 0704-0188

1. REPORT DATE	2. REPORT TYPE	3. DATES COVERED
30 JUN 2005	**N/A**	

4. TITLE AND SUBTITLE	5a. CONTRACT NUMBER
Device Developments for Qubits Using Electrons on a Helium Film	5b. GRANT NUMBER
	5c. PROGRAM ELEMENT NUMBER
6. AUTHOR(S)	5d. PROJECT NUMBER
	5e. TASK NUMBER
	5f. WORK UNIT NUMBER
7. PERFORMING ORGANIZATION NAME(S) AND ADDRESS(ES) **U.S. Army Research Office P.O. Box 12211 Research Triangle Park, NC 27709-2211**	8. PERFORMING ORGANIZATION REPORT NUMBER
9. SPONSORING/MONITORING AGENCY NAME(S) AND ADDRESS(ES)	10. SPONSOR/MONITOR'S ACRONYM(S)
	11. SPONSOR/MONITOR'S REPORT NUMBER(S)

12. DISTRIBUTION/AVAILABILITY STATEMENT
Approved for public release, distribution unlimited.

13. SUPPLEMENTARY NOTES
The original document contains color images.

14. ABSTRACT

15. SUBJECT TERMS

16. SECURITY CLASSIFICATION OF:			17. LIMITATION OF ABSTRACT	18. NUMBER OF PAGES	19a. NAME OF RESPONSIBLE PERSON
a. REPORT	b. ABSTRACT	c. THIS PAGE			
unclassified	**unclassified**	**unclassified**	**UU**	**19**	

faster than required by anticipated relaxation times. However, Dykman has shown that there is another limit on the switching speed[3].

The qubit behavior that cannot be easily simulated numerically is the dephasing and relaxation due to coupling to the outside world. As in all quantum information systems, the relaxation times resulting from this coupling determine whether the qubits will be useful. Theoretical analysis of the coupling mechanisms and calculation of the relaxation times was done by Platzmann and Dykman[4]. They showed that the dominant relaxation mechanism on ^{4}He films is coupling between electrons and ripplons and that at 10 msec the dephasing time is long enough to satisfy the criteria for quantum error correction. No theory has yet been developed for using a film of ^{3}He nor have experimental measurements been made. However, relaxation times may be longer on ^{3}He.

2 Instrumentation requirements:

In order to use these quantum states for qubits, microwave radiation at the resonance condition must be applied selectively to individual electrons. A single microwave source at a fixed frequency is used to excite the electrons, so that to selectively excite specific electrons they must be Stark shifted by a static electric field into resonance with the microwaves. Currently we use 140 GHz microwaves. In order to apply Stark shifts to selected electrons, they must be constrained horizontally over microelectrodes that provide the Stark shift field. We describe the microelectrode structure that we have developed for this purpose. In order to provide a replenishable supply of electrons, a source of low energy electrons is required that can operate at temperatures below 1 K without heating the entire system above about 500 mK. A significant portion of the distribution of energies must be below 1 eV since, above that energy, electrons will penetrate the liquid helium rather than remaining on the surface. We describe the porous silicon diode that we developed for the purpose. Our method for detecting the quantum state of individual electrons, after completion of a logic operation, is to apply an electrostatic "pulling field" that extracts all excited state electrons while leaving ground state electrons in place. We then apply a pulling field large enough to extract ground state electrons to one microelectrode at a time to determine which qubit was in the ground state at the end of the operation. This required fabrication of single electron detectors that operate with very high efficiency at mK temperatures. We developed superconducting micro-bolometers for this purpose.

2.1.1 The electron source

2.1.2 Porous silicon diode

The porous silicon (PS) diode provides the required low energy electrons at temperatures below 100 mK with very little heating of the system. Details of its development and operation have been published[5]. It is fabricated by electrochemical etching of crystalline, doped Si in a hydrofluoric acid electrolyte. A thin Au film is deposited on top of the porous area to allow application of a DC bias (V_{PS}) that causes a current to flow through the diode (I_{PS}) and to emit electrons into the vacuum (I_E). A Au film thickness < 5 nm is not continuous when deposited on the PS so that it does not produce a diode. A thickness >10 nm, prevents emission of electrons. Electron emission had not previously been

measured in the mK temperature range. We found that emission efficiency (I_E/I_{PS}) is independent of V_{PS} and increases with decreasing T and can be as high as 10^{-4} at its low temperature limiting value. The efficiency also depends on the duration of the V_{PS} pulse and peaks between 3 and 5 msec. For repeated pulses the emission decreases as the number of pulses increases unless a reverse bias is applied between pulses. In the latter case the efficiency and emission current is stable for an arbitrarily large number of pulses and independent of repetition rate for rates as high as 2/second. At higher rates the emission decreases but is high enough for our purposes up to 10^3/second. From the extrapolation of the curve fits at measurable currents, we estimate that ~2500 electrons/ pulse are emitted for V_{PS}=15 V and pulse width 4 ms. Heating from these pulses is negligible even below 100 mK.

We have obtained stable emission with liquid ^{4}He and ^{3}He films on the diode surface. In the case of ^{4}He, no change in emission is observed when the temperature is lowered below the superfluid transition temperature of 2.2 K. However, I_E with either ^{4}He or ^{3}He is about 5–10 times smaller than emission in vacuum for the same V_{PS} and V_{acc} values. The energy distribution of the emitted electrons is shown in Figure 1. It is unusual and very desirable for our application in that it has a high density at energies below 0.1 eV.

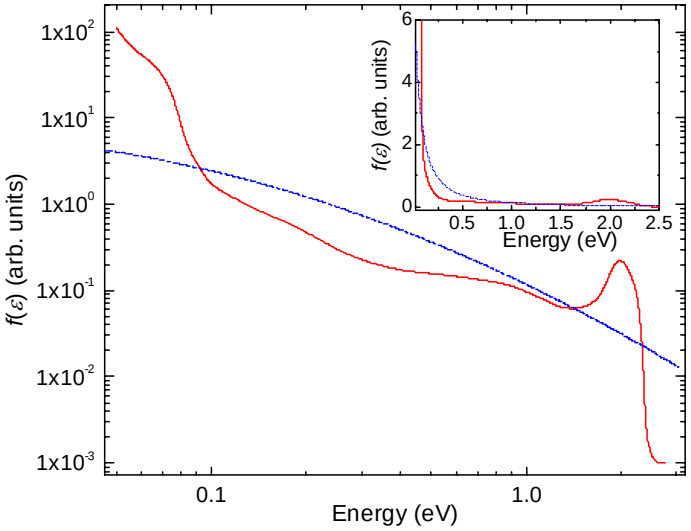

Figure 1. Relative numbers of emitted electrons as a function of energy from the PS Diode operating at 77 K. The main plot shows the distribution in log scale while the inset shows the same distribution in linear scale. A normal distribution with μ = 0, σ = 1.6, and the scale parameter m = 0.14 is included for comparison.

The diode has properties that make it difficult to use for development work which requires frequent cycling between room temperature and cryogenic temperatures. The electron emission at cryogenic temperatures is reduced or eliminated if the diode is exposed to He gas at room temperature. It can also be damaged by emitting electrons at room temperature so that we normally operate it only after cooling to LN_2 temperature. Consequently, the sample chamber cannot be leak checked until the system has been cooled to LN_2 temperature. This leads to wasted time for development work when it requires many thermal cycles to room temperature and requires leak checking on each cooldown.

2.1.3 Pulsed thoriated tungsten filament.

As a consequence we have also developed thermionic emission from thoriated tungsten wire using short pulses. We found that the wire glows with a pulse as short as 24 msec with a current of 120 mA. This corresponds to about 1 mJ of energy in the filament. Much smaller energies are required to emit electrons in the small numbers that

we require. Both devices have been installed simultaneously in some of the test experiments.

2.2 Single electron detectors.

Our technique for detecting the ejection of individual electrons uses superconducting transition edge microbolometers. These are microfabricated in the form of a meander pattern as shown in Figure 2.

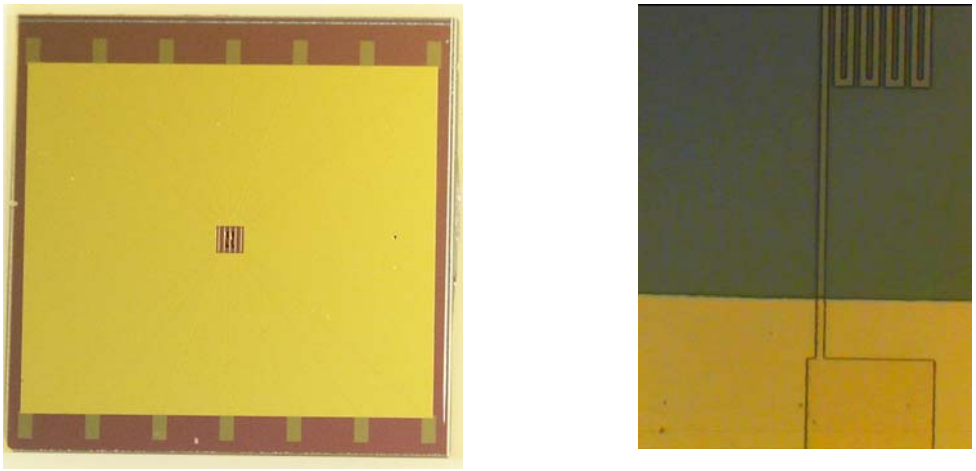

Figure 2. Photograph of the original test microbolometers. Left side is the complete 1.4 cm X 1.4 cm chip showing the ground plane and contact pads for the bolometers located in the opening of the ground plane. The right side shows detail of an edge of the detector meander pattern.

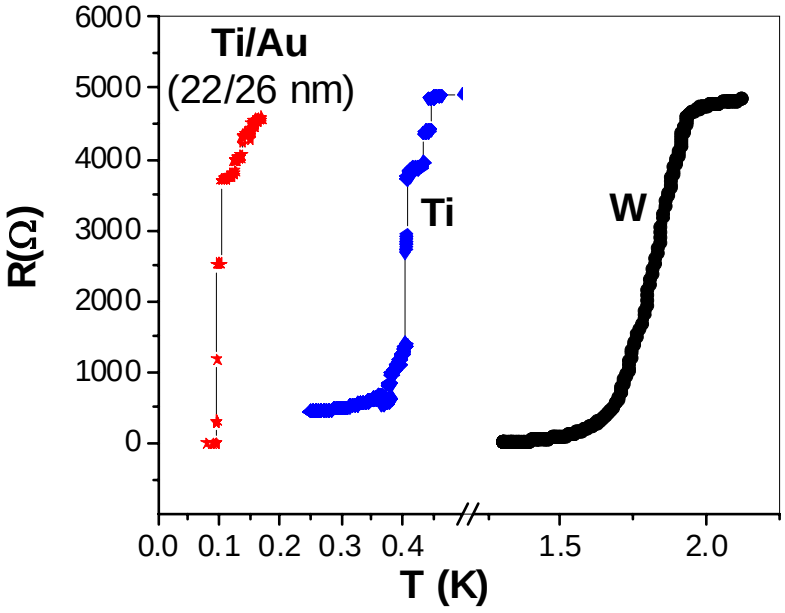

Figure 3. R vs. T for three different detectors from thin films of W, Ti, and Ti/Au. The latter used a 22 nm thick film of Ti with an over layer of 26 nm of Au. The proximity effect of the Au reduces the T_C of the Ti film.

In order to be able to detect single electrons with less than 10 eV of energy we need devices with critical temperature < 100 mK. During logic operations we want the system to be at 10 mK or below. If the sample chamber is heated above about 200 mK the system will require many minutes to cool back to 10 mK for the next logic operation. Consequently, we want the detectors to have T_C as close as possible to 10 mK. In previous work we have used magnetic field bias

to adjust the critical temperature of Zinc bolometers[6] and that technique will also be used in this work when required. However, in order to obtain the sharpest transition (highest sensitivity) and to use the lowest magnetic field bias we have aimed for T_C of about 100 mK in zero field. Superconductors which have very low T_C in bulk, such as W (bulk T_C = 0.015) and Ti (bulk T_C = 0.39), have much higher T_C in thin films so that techniques to lower it are needed. We first tried using ion implantation of impurities in Ti films but found that difficult and expensive. Recently, we also tried W using published techniques[7] for adjusting T_C but the prescription did not work in the sputtering system at UCSD. Our most successful technique has been placing a layer of normal metal (Au) on top of Ti. This uses the "proximity effect" in which the normal metal in contact with the superconductor lowers its critical temperature for a small distance from the interface. Resistance vs *T* is shown in Figure 3, for three different thin film devices fabricated in the pattern of Figure 3.

In order to direct the electrons to the detector we bias it positive. This means that the leads must be electrostatically shielded so that electrons will be attracted only to the detector meander pattern. Therefore, after the meander pattern and the leads are deposited, additional photolithographic steps are used to cover the leads with an insulator and a metallic ground plane, with an opening over the meander pattern and over the contact pads as shown in Figure 2. The most reliable procedure has been to do the entire fabrication using rf sputtering, using SiN as the insulator. We have also used TiO_2, and PMGI as the insulator. PMGI made the fabrication simpler but the process using it did not produce reliable devices.

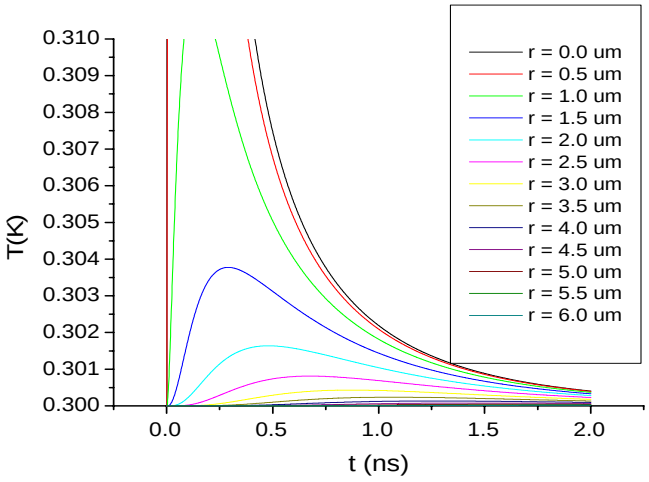

Figure 4. Simulation of propagation of the temperature rise resulting from deposition of heat at a point at time 0.

Part of the background work for fabricating the devices was an attempt to simulate the propagation of the temperature rise resulting from deposition of heat at a point in, or near, the meander pattern. The simulation assumes perfect thermal contact between ground plane, insulator and substrate but bulk thermal conductivity within each. The results of the simulation are shown in Figure 4. Temperature as a function of time after deposition of the energy is plotted for a range of distances from the point of deposition.

2.3 Microstructure for trapping electrons.

The microelectrodes are in the form of posts approximately 1.5 μm tall and 200 nm in diameter with center to center spacing of 500 nm. The dimensions were selected for a helium film thickness such that the electrons would be 0.5 μm above the top of the electrodes. The spacing between the electrodes was selected to provide an interaction between qubits so as to yield a 1 GHz swap frequency. Leads are connected to each electrode so that the electric field above each can be adjusted independently. A ground plane, covering the leads to the electrodes is required (as for the detectors) to shield the electric field from the leads so that electrons will be trapped only over the electrodes.

The structure shown in Figure 6 is fabricated using photolithographic techniques[8]. Starting with a 10 cm Si wafer, a 2 μm insulating layer of SiO^2 is deposited, followed by a 0.5 μm layer of SiN. Both are deposited using plasma enhanced chemical vapor deposition (PECVD). Nine dies in the pattern of Figure 6 are then deposited using a 5X

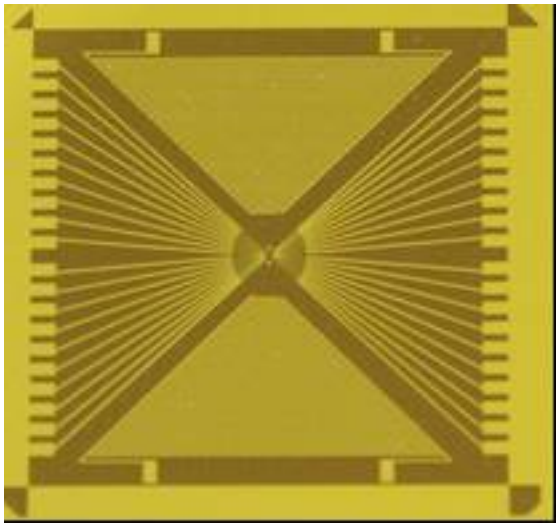

Figure 6. 15 mm square chip showing Leads for the microelectrodes prior to deposition of the insulator and ground plane and microelectrodes. After fabrication of the electrodes, the dies are diced around the edges so as to separate the contact pads. The upper and lower triangles are interleaved lines of a capacitor for measuring the thickness of the helium film.

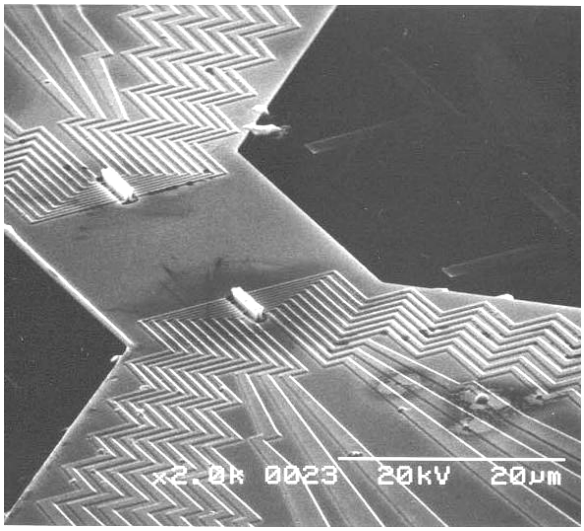

Figure 5. SEM photo of the central portion of the original micropost chip. Posts are visible protruding through the two openings in the ground plane. The profile of the leads to the electrodes propagates through the insulating layer and the ground plane. In this sample the electrodes were over plated so that they are shaped like mushrooms and joined together at the top.

stepper. In the standard manner a layer of Ti is evaporated first, to provide adhesion to the SiO2. Local alignment marks, visible on either side of the ground plane in Figure 5,

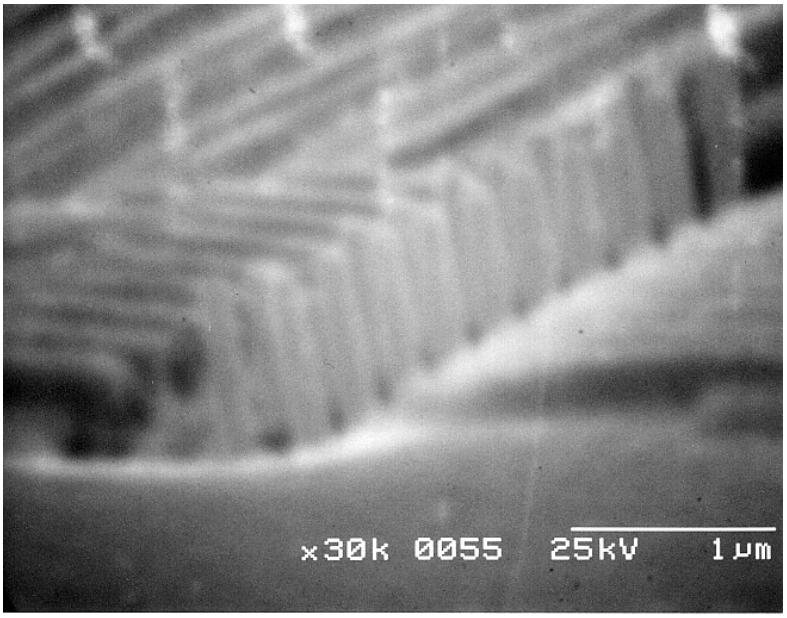

Figure 7. SEM image of properly plated microelectrodes.

were written along with the leads to provide accurate alignment of the electron beam pattern in the subsequent steps. After lift-off, an e-beam resist, ZEP 520A, is then spun onto the wafer and the fine leads at the center of the pattern (Figure 6) are written with the electron beam. Prior to writing with the e-beam, a 10 nm thick layer of gold is deposited on the resist to prevent charge buildup during the writing process. The e-beam leads have complex zigzag patterns, shown in Figure 5 , so that the dosage is varied from place to place to avoid distortion from the proximity effect. Current techniques at the NINN facility in Santa Barbara now allow us to write simpler patterns for which this adjustment is not necessary.

Next, after lift off of the ZEP 520A, insulator and ground plane are deposited, again using photolithography in the stepper. The next steps are deposition of 0.5 μm insulating SiN layer over the lead wires, deposition of a metal ground plane and creation of small rectangular openings in SiN and ground plane layers through which the microelectrodes will be fabricated in the final step. Two, slightly different processes have been used for these steps. In the first process that we tested, we used a bilayer negative photo-resist. The mask exposes the upper and lower triangles of Fig. 5 (the in-plane capacitors) as well as the small openings for the tips of the electrodes (Figure 5). A single layer resist process is not suitable for sputter deposition of SiN because of side wall coverage during sputtering which makes liftoff impossible. In a bilayer resist process, the under layer is slightly over developed to provide overhang of the top layer. The under layer thickness and the overhang are chosen such that even after depositing 0.5 μm thick layer over the resist, enough gap between the overhang and the substrate remains to allow solvents to reach the bottom of the resist for liftoff. As the openings in the ground plane and SiN layers are only 1.3 μm wide by 5.5 μm long, the mask for this exposure requires very

accurate stepper alignment using the local marks shown in Figure 5. The mask is therefore aligned within 0.35 μm to provide sufficiently accurate centering of the columns within the openings. Several attempts at alignment are required to achieve this precision.

After developing the resist, a 500 nm thick SiN insulating layer is deposited by magnetron sputtering. Sputtering proceeds at sufficiently low temperature so that it does not harden the resist. SiN was chosen as the insulating material because of its high breakdown voltage and good adhesion to the gold wires. 100 nm of Pt is then deposited for the ground plane without breaking the vacuum. Finally, lift-off removes the SiN and Pt over the in-plane capacitors and leaves the two small openings for the electrodes.

A second method is based on a more reliable two step process for depositing the SiN/Pt layers. In the first step, we deposit 500 nm SiN layer on the entire wafer using PECVD process. A thin layer of positive resist is then spun onto the wafer and exposed with the positive mask pattern for the ground plane using the optical stepper. A 100 nm Pt layer is then deposited by e-beam evaporation. Careful local alignment of the stepper is required only for this second step. After liftoff and cleaning, Reaction Ion Etching (RIE) is used to remove the unwanted SiN in the two small ground plane openings and in-plane capacitor regions. In the RIE process using SF_6 and O_2, no other masks are necessary because the Pt ground layer and the Ti/Au lead wires etch sufficiently slowly to act as a mask. During RIE etch, the oscillations of the reflection intensity of a laser spectrometer is used to monitor the etch process.

The final step, is the electro-plating process to grow uniform cylindrical columns at the tip of each lead exposed in the ground plane opening. To accomplish this, a layer of PMMA 0.6 to 0.8 μm thick is spun uniformly on to the wafer. The e-beam writer, operating at 50 keV, is then used to write holes through the resist to the ends of the lead wires exposed in the small openings of the ground plane. Due to the capillary action, the resist fills these small openings completely resulting in the desired 1.2 to 1.4 μm thickness where the columns are grown. The dosages and developing times to fabricate the electrodes were previously determined by using a range of both on dies covered by a solid gold film. Over exposure or over developing resulted in posts in the shape of cones with the broad base at the bottom. Underexposure or underdeveloping resulted in posts in the shape of inverted cones. The best dosage was to be 1200 $\mu C/cm^2$ for the columns separated by ~ 0.5 μm and yields holes about 200 nm in diameter. The beam is aligned on each ground plane opening on each die using the local alignment marks. The optimal developing time for the holes is five minutes in MIBK:IPA (1:3) in an ultrasonic bath.

The wafers are diced prior to developing so that developing of the PMMA and the gold plating are performed one die at a time. In this way, errors in developing or plating times effect only one die rather than the entire wafer. After developing, the dies are immersed in the gold plating solution heated to 65 ºC. A 1 cm^2 test strip is also connected to the anode and immersed in the bath. The total current density is adjusted to 2.5 mA/cm^2. Typical plating time is 2.5 minutes. All of the microelectrode leads are shorted together for this process, around the perimeter of the chip, as shown in Fig. 5 and only the tips of the e-beam leads in the ground plane opening are exposed to the plating solution. The plating time is critical, and it depends on the surface roughness of gold leads which results from the RIE etching and can not be controlled accurately. Plating for too long overfills the holes leading to a mushroom shape on top of the columns which can

electrically short all of the columns together. Plating for too short a time results in columns that are too short. A complete description of the entire process is provided in reference 8.

2.4 Numerical analysis of electric fields.

The geometry of the electric field from the ground planes and microelectrodes has been computed using commercial software (FLEXPDE). The results provide the voltages required to produce the desired horizontal restoring force as well as the desired Stark shifts and field gradients in the z direction. The results also confirmed approximate calculations showing that fundamental oscillation frequency in the horizontal plane will be of order 1 GHz for the anticipated operating conditions.

2.5 Microwave system

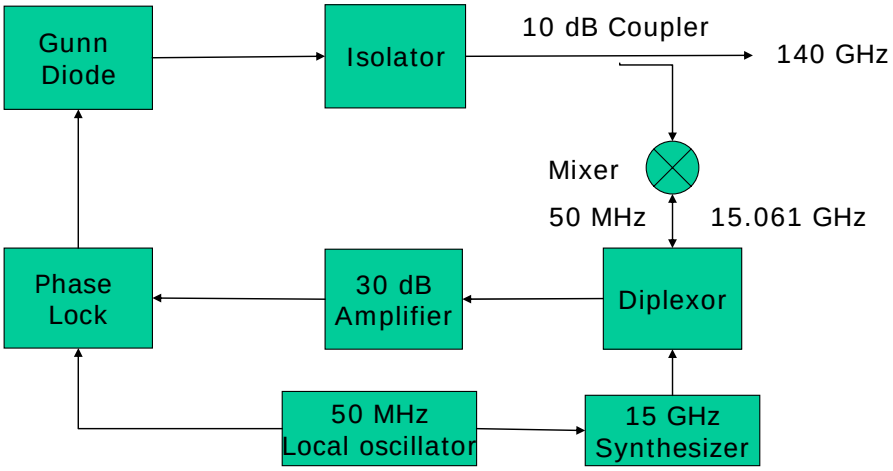

Figure 8. Block diagram of the 140 GHz phase locked loop signal source. The 140 GHz output is then gated by a PIN diode to produce the rf pulses to operate the single qubit gates.

A schematic diagram of the 140 GHz microwave system is shown in Figure 8. The output of the system is gated by a PIN diode to produce the rf pulses required for qubit gate operation. A detected pulse is shown in Figure 9. The rise time displayed is limited by the detector response into a 50 Ω load. The actual rise time of the microwave power is much faster. Although it is still "adiabatic" in terms of the solutions to the Schrodinger equation, other considerations may require that the rise time be increased by shaping the gate pulse. The detector is calibrated only for operation into a 1 MΩ load in which case the detector output is 700 mV with a rise time of several msec. Coin silver waveguide is used through regions that are at uniform temperature. Stainless steel is used between room temperature and 4.2 K and between 4.2 K and the sample chamber. The attenuation through the waveguide, *in situ*, reduces the power to a level below the calibration range of the detector but is still sufficient to obtain a 90º pulse with a width of order 1 μsec. The waveguide is vacuum sealed at room temperature and at the sample chamber walls by clamping .025 mm thick Mylar sheet between microwave flanges. The attenuation due to the Mylar is too small to measure with our detector.

2.6 The complete assembly:

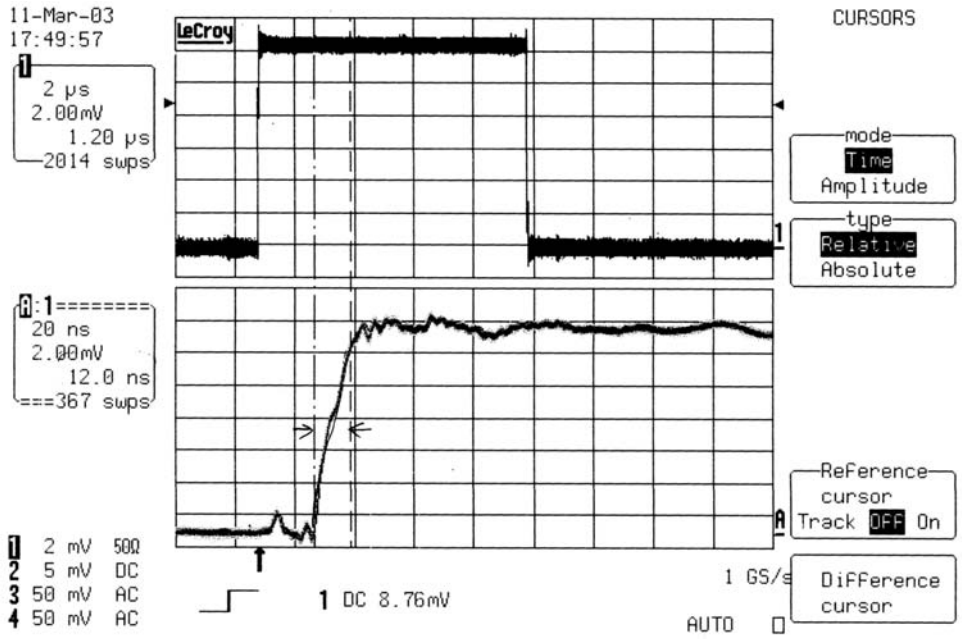

Figure 9. Printout of scope trace of detector output from an 8 µsec pulse of 140 GHz power. Upper trace is the entire pulse displayed at 2 µsec/division and 2 mV per division. Lower trace is expanded to show the rise time, at 20 nsec/division.

The original plan for the assembly of the three components, is illustrated in Figure 10. The PS diode electron source is at the top facing down. Electrons will pass through a hole in the detector chip and end up on the helium film covering the microelectrode chip at the bottom. Microfabrication of the detector chip with small holes on either side of the detector was successful but required too much clean room time. Currently we are using a different scheme described below.

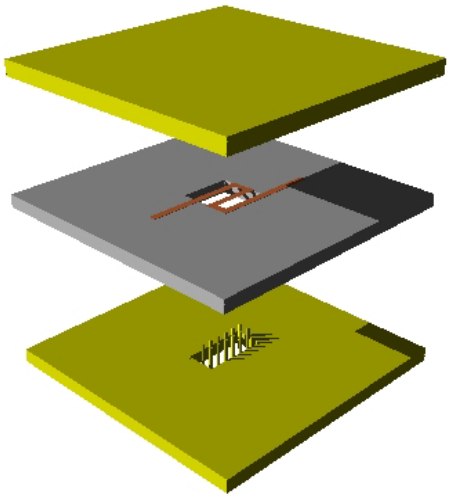

Figure 10. Arrangement of the three components without the waveguide. Top plate is the electron emitter, central plate with hole for passage of electrons, bottom plate with microelectrodes for trapping electrons on the helium surface which will be 0.5 µm above the top of the electrodes.

3 Construction of the sample chamber

The sample chamber with WR8 waveguide and with the three components is shown in the drawing of Figure 11. The upper and lower surfaces of the waveguide are machined away in the central portion of the sample chamber. So that the ground planes of the detector and microelectrode chips become the conducting surfaces of the waveguide. The waveguides are isolated from apparatus ground so that their potentials can be adjusted for optimal trapping and then releasing of electrons.Microwave attenuation through this section is less than 10 db.

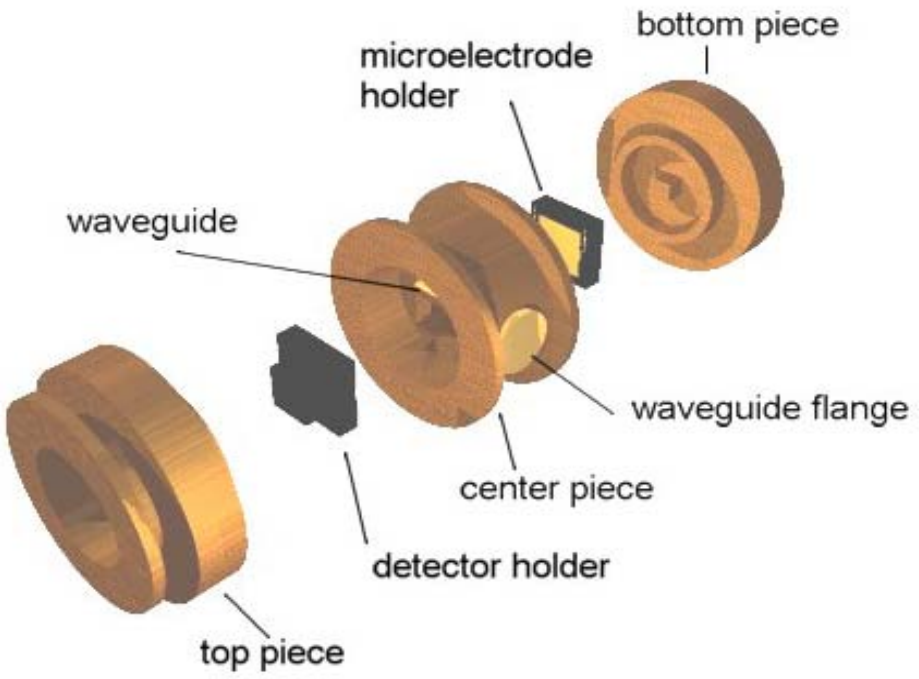

Figure 11. Drawing of the sample chamber including the waveguide, electron source, detector, and microelectrode chip.

The waveguide is vacuum sealed (superfluid tight) at the flanges on both sides of the sample chamber with .025 mm thick mylar film, clamped between the flanges.

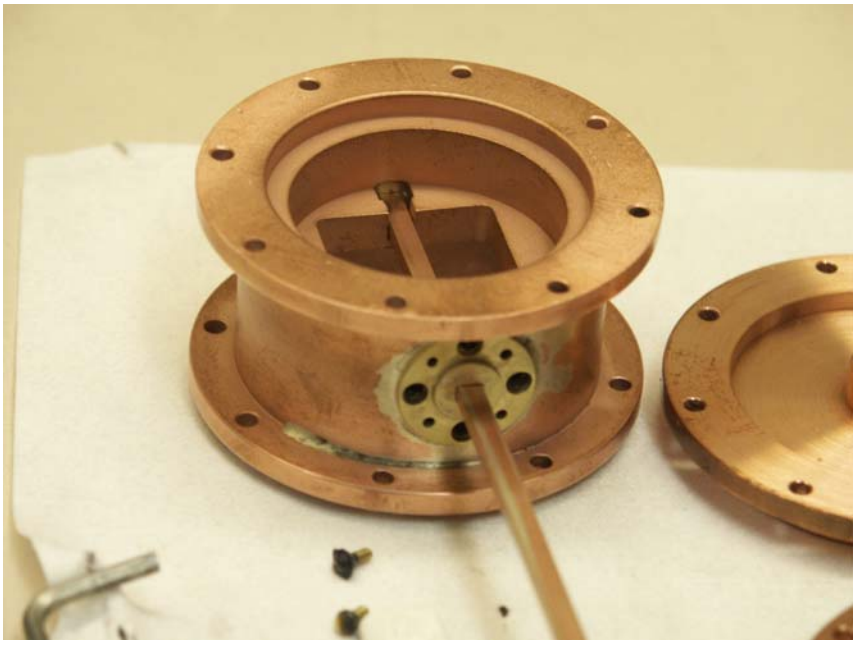

Figure 12. Photograph of sample chamber showing waveguide. The chip assemblies on the top and bottom plates are not shown.

4 Measurement of film thickness: In-plane vs parallel plate capacitor

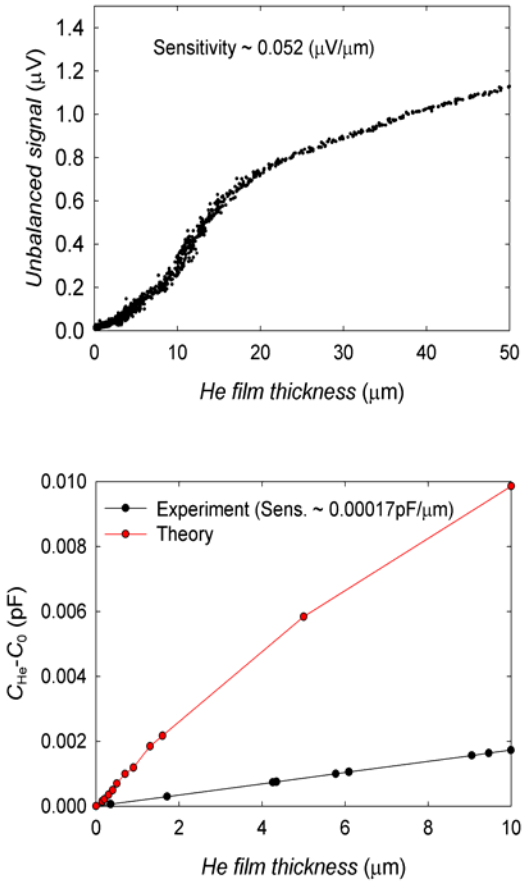

Figure 13. Capacitance bridge signals due to the helium film as a function of film thickness, from the in-plane capacitor.

The original design intended to use the in plane capacitor (interleaved lines in Figure 6) to measure and control the film thickness. Capacitance to the substrate and materials underneath the substrate reduced the sensitivity far below its anticipated value so that we were able to obtain about 30 times greater sensitivity with horizontal parallel plates without employing more sensitive capacitance bridge techniques. The convenience and additional sensitivity of the parallel plates was then used for experiments described below. In the ultimate configuration, discussed below, much less precise measurement of the film thickness is required.

5 Test for trapping and ejection of electrons

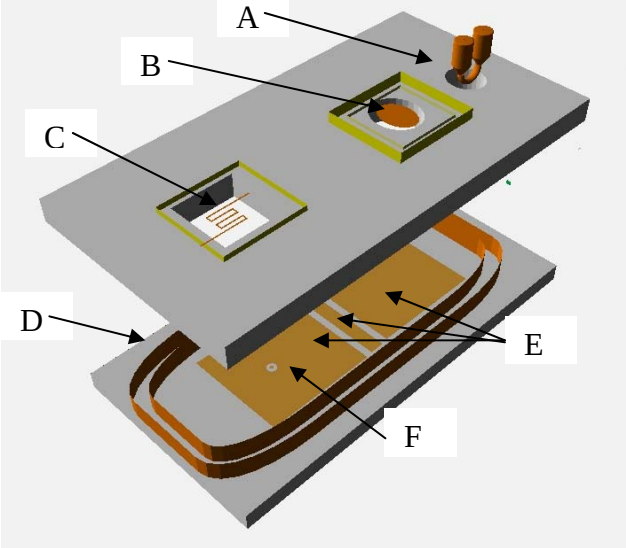

Figure 14. Configuration of system for measuring trapped electron density and for detecting electrons ejected from the helium surface. A, discharge electron source. B, Porous silicon diode source,. C, TES detector. D, ring capacitor to measure helium film thickness and to apply horizontal confining field. E, in-plane capacitor plates to measure electron density by measuring conductivity through electrons on the helium surface. F, small disc to eject a small fraction of the electrons on the helium surface over the left capacitor plate. The potential of all metal surfaces on the lower substrate can be adjusted independently.

In our first attempt to detect electrons ejected from all 40 of the microelectrodes we obtained no signal. Subsequent tests showed that the PS diode had been poisoned with helium gas at room temperature so that no electrons were ejected. We then constructed a sample system as shown in Figure 14 to allow several test experiments. The gray

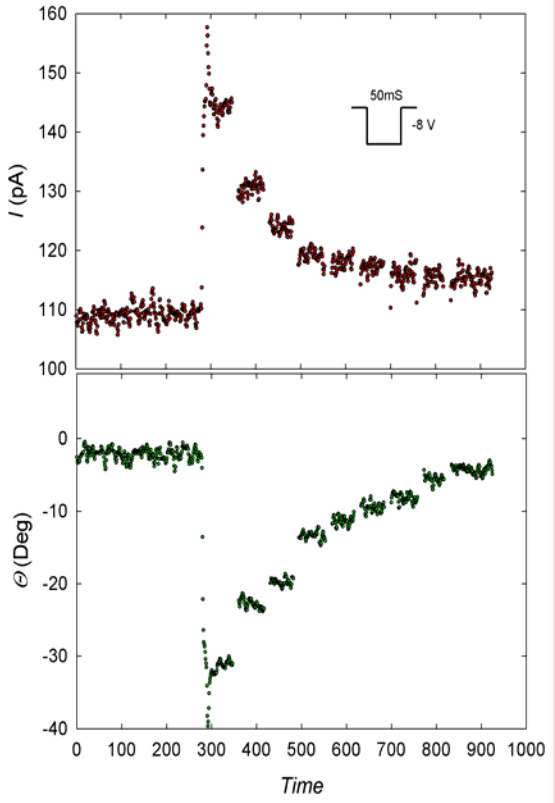

Figure 15. Amplitude and phase of the current through the 2D electron layer on the liquid helium. Each step represents the release of a few hundred electrons trapped on the surface of liquid helium.

rectangular objects represent glass microscope slides that were used as substrates and mechanical holders. The large plates in the plane of the lower substrate, (E), are used to measure the impedance due to electrons on the surface of the helium film. This allowed us to determine unambiguously that we had collected electrons and to measure the density of the 2D electron gas. The metal dot at the center of the small hole, (F), is connected to a wire passing through the substrate so that electrons can be trapped over the dot and released. The two ring plates , (D), are used to measure the thickness of the helium film. (A) represents the thoriated tungsten electron source. (B) is the PS diode source. (C) is one of our microbolometer detectors.

The phase and amplitude of the impedance through the electrons is shown in Figure 15 as a function of time while applying negative pulses to the thin center plate of Figure 14 (E). The highest density is assumed to correspond to about 10^8 cm^{-2} since this is the highest density that could be trapped in our previous experiments on bulk helium[2]. The current then scales with the electron density. From this inferred density and the known area of the dot we could estimate the number of electrons over the dot, when it is at the same potential as the large plate surrounding it.

Bolometer signals were observed when negative pulses were applied to the dot, at densities corresponding to as little as a few hundred electrons on the dot. They were consistent with previous experiments indicating that we should be able to observe a single electron with energy ~ 10 eV.

At a later time, electrons were trapped over a microelectrode chip (Figure 5) in which 4 of the microelectrodes were shorted together (due to overplating) and the others were missing. The meander patterns on either side of the microelectrodes were shorted together so as to form capacitor plates analogous to those of Figure 14E. These were used to monitor the deposition of electrons and to sweep electrons across the electrodes located in the central area of the chip. The detector signal resulting from the application of a 1 Volt pulse to the electrodes is shown in Figure 16. We were unable to determine how many electrons were released in this experiment.

6 Development since termination of ARDA funding

The last experiment described above also revealed an instability in the system at temperatures below about 200 mK. It appeared in the form of very low frequency oscillations of the electron current that could be triggered by tapping on the Dewar. We had observed a similar phenomenon in previous work[2]. We assume that it is a mechanical oscillation of the bulk liquid helium in the cell when the damping becomes very small.

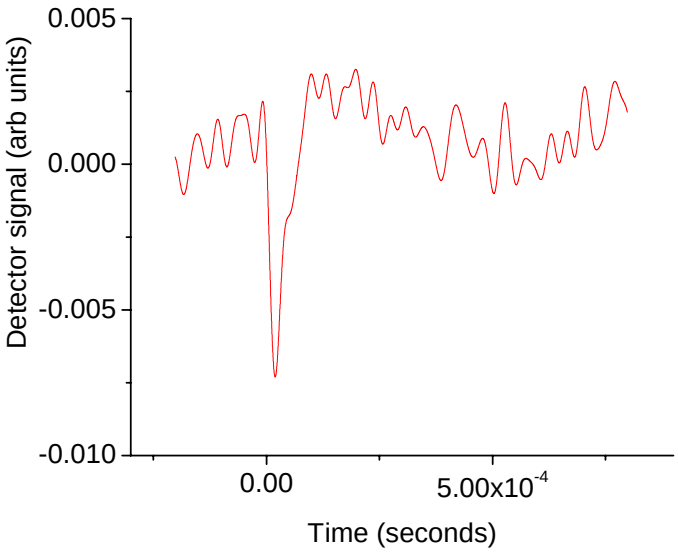

Figure 16. Detector signal from the release of electrons trapped over 4 microelectrodes shorted together due to overplating.

Rather than attempting to clamp this mode and reduce vibrations in the cryostat we decided to eliminate the bulk liquid and use only a film. The thickness of the film is determined by the capillary force in a channel 10 μm wide. The channel is fabricated by writing a long closed loop with the e-beam writer on top of the ground plane surrounding the microelectrodes. After developing, a wall is created by electroplating into the loop. The wall is fabricated to a height 0.5 μm. This is the technique used by our colleagues

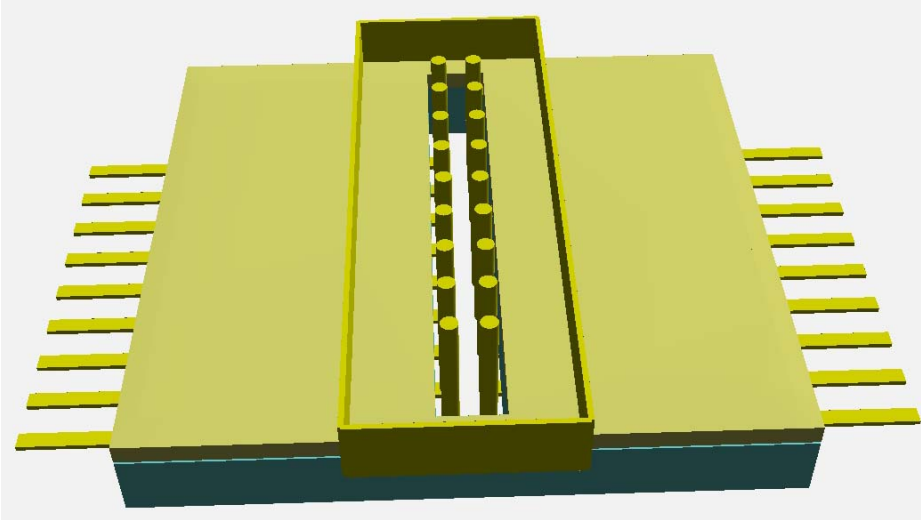

Figure 17. Schematic drawing of the channel to set the film thickness without bulk helium in the chamber. The channel walls are fabricated at width 10 μm, height 0.5 μm higher than the microelectrodes, and 100 μm long extending on both sides of the opening in the ground plane.

in Great Britain for their approach using SET detectors.

We have continued to work on detector development. We currently fabricate only a single meander line rather than the original five so that the opening in the ground plane is smaller. Rather than continue to try to fabricate detectors with lower T_C we are going to use a small magnetic field to adjust the T_C of a Ti detector in the manner that was used in previous work in this laboratory[6].

---

[1] C.C. Grimes, T.R. Brown, M.L. Burns, and C.L. Zipfel, "*Spectroscopy of electrons in image-potential-induced surface states outside liquid helium*", Phys. Rev. B **1**3, 140-147 (1976).

[2] G.F. Saville, J.M. Goodkind, and P.M. Platzman, "*Single-electron tunneling from bound states on the surface of liquid helium*", Phys. Rev. Lett. **7**0, 1517-1520 (1993).

[3] L.F. Santos, M.I. Dykman, M. Shapiro, and F.M. Izrailev, ``Strong many-particle localization and quantum computing with perpetually coupled qubits", Phys. Rev. A **71**, 012317 -- 1-18 (2005)

[4] Platzman and Dykman, "Quantum Computing with Electrons Floating on Liquid Helium" Science **284,** 1967 (1999)

[5] S. Pilla, B. Naberhuis, and J. Goodkind, "*A porous silicon diode as a source of low-energy free electrons at milli-Kelvin temperatures*", J. Appl. Phys. **98**, 024508 (2005)

[6] John M.Goodkind, "Interaction of First and Second Sound in Solid 4He: Properties of a Possible Bose Condensate" Phys. Rev. Lett., **89**, 095301 (2002)

[7] A. E. Lita, D. Rosenberg, S. Nam, A. J. Miller, D. Balzar, L. M. Kaatz, and R. E. Schwall, "*Tuning of Tungsten Thin Film Superconducting Transition Temperature for Fabrication of Photon Number Resolving Detectors*" IEEE Transactions on Applied Superconductivity, **15**, 3528 (2005)

[8] S Pilla, X C Zhang, B Naberhuis, A Syschenko, and J M Goodkind, "High Aspect Ratio Micro-Columns to Manipulate Single Electrons on a Liquid Helium Surface for Quantum Logic Bits", to be published in IEEE Transactions on NanoTechnology (2005)